HAL
open science

Ceres2d: a Numerical Prototype for Hc Potential Evaluation in Complex Area

F. Schneider, H. Devoitine, I. Faille, E. Flauraud, F. Willien

To cite this version:

F. Schneider, H. Devoitine, I. Faille, E. Flauraud, F. Willien. Ceres2d: a Numerical Prototype for Hc Potential Evaluation in Complex Area. Oil & Gas Science and Technology - Revue d'IFP Energies nouvelles, 2002, 57 (6), pp.607-619. 10.2516/ogst:2002041 . hal-02043982

HAL Id: hal-02043982

https://ifp.hal.science/hal-02043982v1

Submitted on 21 Feb 2019

HAL is a multi-disciplinary open access archive for the deposit and dissemination of scientific research documents, whether they are published or not. The documents may come from teaching and research institutions in France or abroad, or from public or private research centers.

L'archive ouverte pluridisciplinaire **HAL**, est destinée au dépôt et à la diffusion de documents scientifiques de niveau recherche, publiés ou non, émanant des établissements d'enseignement et de recherche français ou étrangers, des laboratoires publics ou privés.

Oil & Gas Science and Technology – Rev. IFP, Vol. 57 (2002), No. 6, pp. 607-619
Copyright © 2002, Éditions Technip

Ceres2D: A Numerical Prototype for HC Potential Evaluation in Complex Area

F. Schneider[1], H. Devoitine[2], I. Faille[1], E. Flauraud[1] and F. Willien[1]

1 Institut français du pétrole, 1 et 4, avenue de Bois-Préau, 92852 Rueil-Malmaison Cedex - France
2 Geomath SA, 232, avenue Napoléon-Bonaparte, 92502 Rueil-Malmaison Cedex - France
e-mail: frederic.schneider@ifp.fr - herve.devoitine@geomath.fr - isabelle.faille@ifp.fr - eric.flauraud@ifp.fr - francoise.willien@ifp.fr

Résumé — Ceres2D : un prototype de modèle de bassin pour l'évaluation du potentiel pétrolier en zones complexes — Cet article décrit Ceres, prototype de modèle de bassin capable de prendre en compte la compaction des milieux poreux, les transferts de chaleur, la génération et la migration des hydrocarbures. De plus, Ceres a été conçu pour gérer des géométries qui évoluent au cours du temps à la suite des effets de la sédimentation, des érosions, de la tectonique salifère et des déplacements le long des failles.

Une étude avec Ceres comprend trois étapes principales. La première concerne la construction de la section à l'époque actuelle. Ceci est généralement effectué à partir des données sismiques, des données de puits et des données de terrain. La seconde étape est la restauration de la section. Cette phase consiste à déterminer, à partir de la section à l'époque actuelle et pour chaque couche définie sur cette section, les géométries intermédiaires en reculant dans le passé. Les simulations directes constituent la troisième et dernière étape du processus. Et, afin de pouvoir résoudre les équations généralement admises en modélisation de bassin, il nous a fallu développer des méthodes numériques originales basées sur des techniques de décomposition de domaines.

Le prototype a maintenant été utilisé pour l'étude de systèmes pétroliers. Dans un premier temps il a été testé pour des études de sensibilité concernant les perméabilités des failles en Bolivie et dans l'offshore du Congo. Dans le golfe du Mexique, il a permis d'étudier l'impact de la tectonique salifère sur la migration des hydrocarbures. Plus récemment, Ceres a été utilisé dans le cadre du consortium SubTrap dans des zones complexes comme les avant-pays canadiens et ceux du Venezuela. En ce qui concerne ces dernières études, l'implication des géologues structuralistes à toutes les étapes du processus s'est révélée véritablement bénéfique.

Abstract — Ceres2D: A Numerical Prototype for HC Potential Evaluation in Complex Area — *This paper deals with the Ceres prototype which is a basin model able to account for porous medium compaction, heat transfer, and hydrocarbon generation and migration. Furthermore, Ceres was designed to handle changing geometry through time as results of sedimentation, erosion, salt or mud creeping and block displacement along fault.*

The classical flow chart to perform a case study is composed of three main steps. The first step is the building of the present day section. This is generally done with data coming from the seismic interpretation, well data, field data and core data. The second step is the restoration of the section. Thus from the section at present day, the section is restored back in the past for each of the defined layer, and until the substratum is reached. The last step is the forward simulation. And, in order to solve the coupled

equations that are generally used in basin models, we had to develop original numerical methods based on domain decomposition techniques.

The Ceres prototype has now been used to study petroleum systems. It has been used to perform sensitivity studies on fault permeability in the Bolivian foothills and the Congo offshore. In the Gulf of Mexico, it allowed to study the impact of the salt tectonics on the hydrocarbon migration. More recently, the Ceres prototype has been tested, within the frame of the SubTrap consortium, in thrust areas such as the Canadian foothills and the Eastern Venezuelan foothills. For these last case studies, it has been beneficial that structural geologists were involved at all stages of the process.

INTRODUCTION

Basin modeling aims at reconstructing the time evolution of a sedimentary basin in order to make quantitative predictions of geological phenomena leading to pressure generation and hydrocarbons accumulations. It accounts for porous medium compaction, heat transfer, hydrocarbon formation and migration (*e.g.* Schneider *et al.*, 2000b).

Today's state-of-the-art sedimentary basin models are able to handle relatively simple geometries resulting from deposition, erosion and vertical compaction. Two main areas however are insufficiently or not at all treated:

– Basin geometry is often not precise enough. Most basins are cut by faults with significant offsets. In addition, basin geometry may be affected by the creeping of salt or mud which in turn may lead to the formation of diapirs.
– Fluid flow and convective heat transfer do not handle the permeability evolution of faults correctly. A fault can be pervious or acts as a seal, and it can change its behavior through time.

The aim of the Ceres project was to build a prototype that is able to simulate three-phase flow in a 2D section of a basin, whose geometry changes due to deposition, compaction, erosion of the sediments, salt or mud creeping, and blocks displacement along faults.

In the first part of the paper, Ceres modules are presented according to the classical work flow used to perform case studies. The second part of the paper is dedicated to a quick review of some cases performed with Ceres during the last years.

1 CERES PROTOTYPE

The software is composed of several modules. The main modules are a section editor, a restoration module and a forward simulation simulator. The other modules are a chronostratigraphy editor, a lithology editor, a kerogen editor, fluid editors, a mesh editor, a run editor and visualization modules. All these modules are managed by a study browser.

1.1 Edition of the Initial Section

The initial section is composed of a chronostratigraphic column and a 2D cross section. In the study browser, this first composite object is represented by the root of a tree. The number of horizons, the corresponding number layers, the ages of the horizons, and the values of the eustatism level are edited with the chronostratigraphic editor.

The section can be edited directly from scratch or its geometry can be imported from other softwares. It is recommended, at this stage to use a structural software (*e.g.* Locace) that is able to balance the section. The edition of the section is split into three steps. First, the geometry of the section is defined *(Fig. 1a)*. Second, the geological attributes are affected. These attributes may be horizon, fault, section boundary, facies change limit. At this stage a decollement level is defined by superimposing an horizon with a fault. At the end of this second step, the section is filled with the lithologies *(Fig. 1b)*. The third step of the edition of the section, is the numerical step. At this stage, the blocks, which represent the smallest kinematics units, are defined *(Fig. 1c)*. Then, each of the blocks is gridded *(Fig. 1d)*. One specificity of the gridding is that each block holds its own grid with no constraint coming from the other blocks. The faults are not gridded in the initial section because their grids are created dynamically during the forward simulation.

The initial section *(Fig. 2)*, once edited, holds the upper mantle, the ductile lower crust, the brittle upper crust and the considered sedimentary part. The faults can exist in the sediments and in the brittle upper crust; they may be rooted at the interface of the brittle upper crust with the ductile lower crust or at predefined decollement levels.

1.2 Restoration of the Section

Once the edition of the initial section is terminated, a backward process, which includes a kinematics restoration, backstripping, and thickness modification, allows determining the input data for the forward calculator. During the backward process, all the periods defined in the chronostratigraphic column should be restored. For this step, it is recommended, especially for complex area, to use a structural forward model (*e.g.* Thrustpack) in order to constrain the geometry through time and to provide a reliable estimation of the eroded parts. At the study browser level, a restoration scenario from the initial section to the final section, only composed of the basement, is represented by a

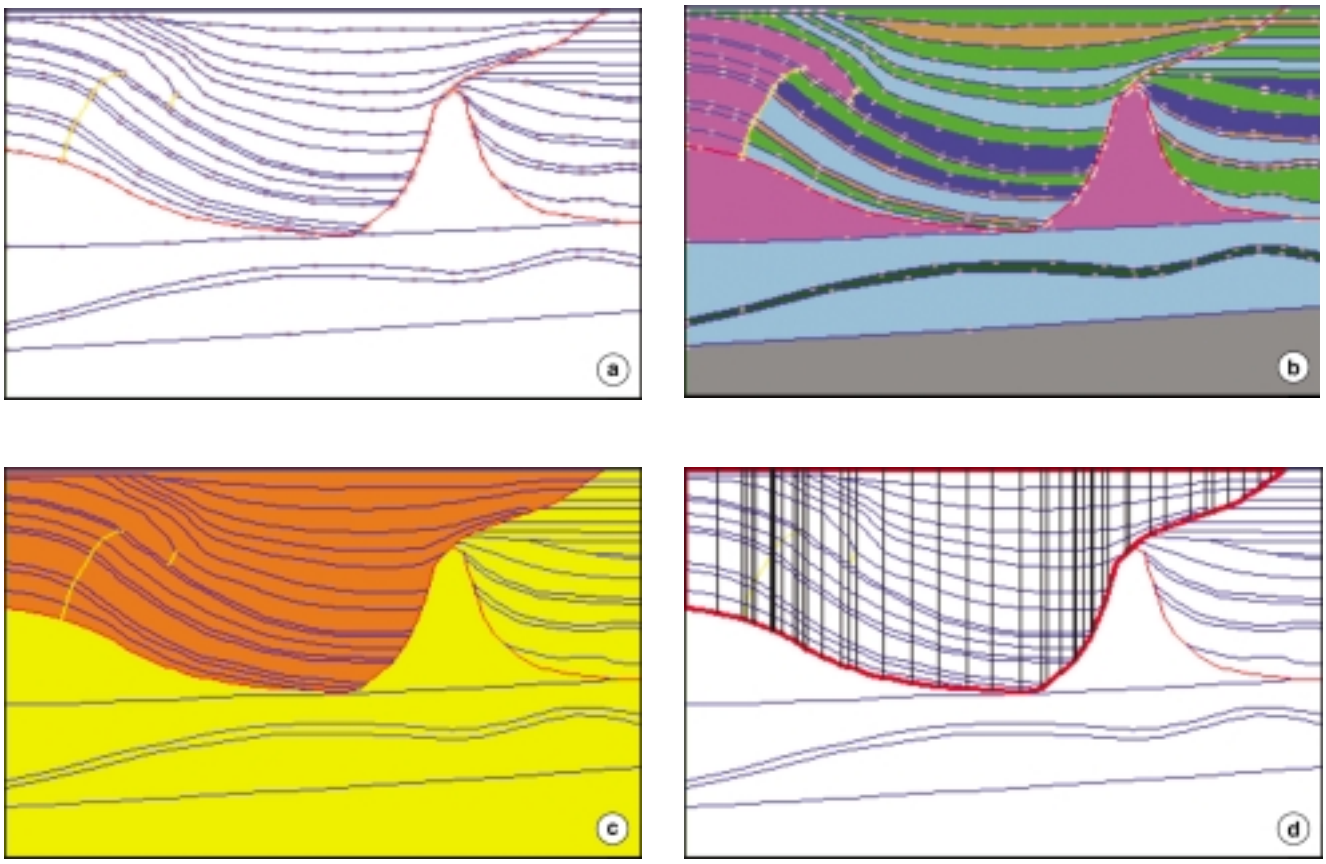

Figure 1

The main steps of the section editor are: (a) edition of the geometry; (b) edition of the geology; (c) creation of the kinematic blocs; (d) building of the grid for each bloc.

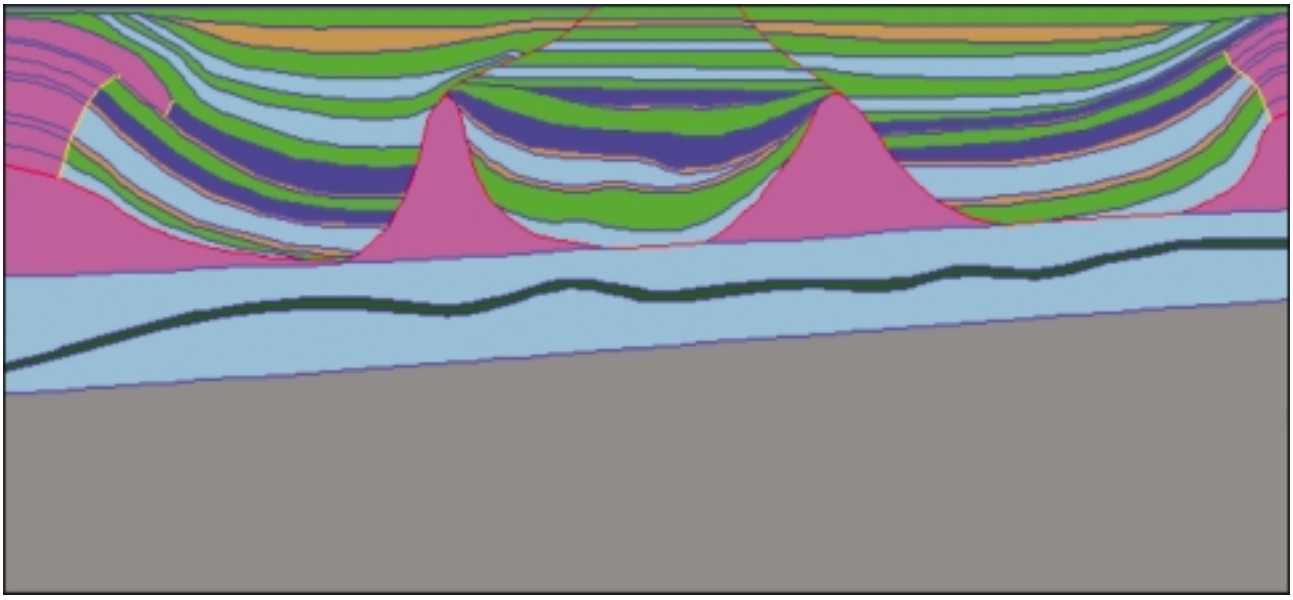

Figure 2

Resulting section at the end of the edition.

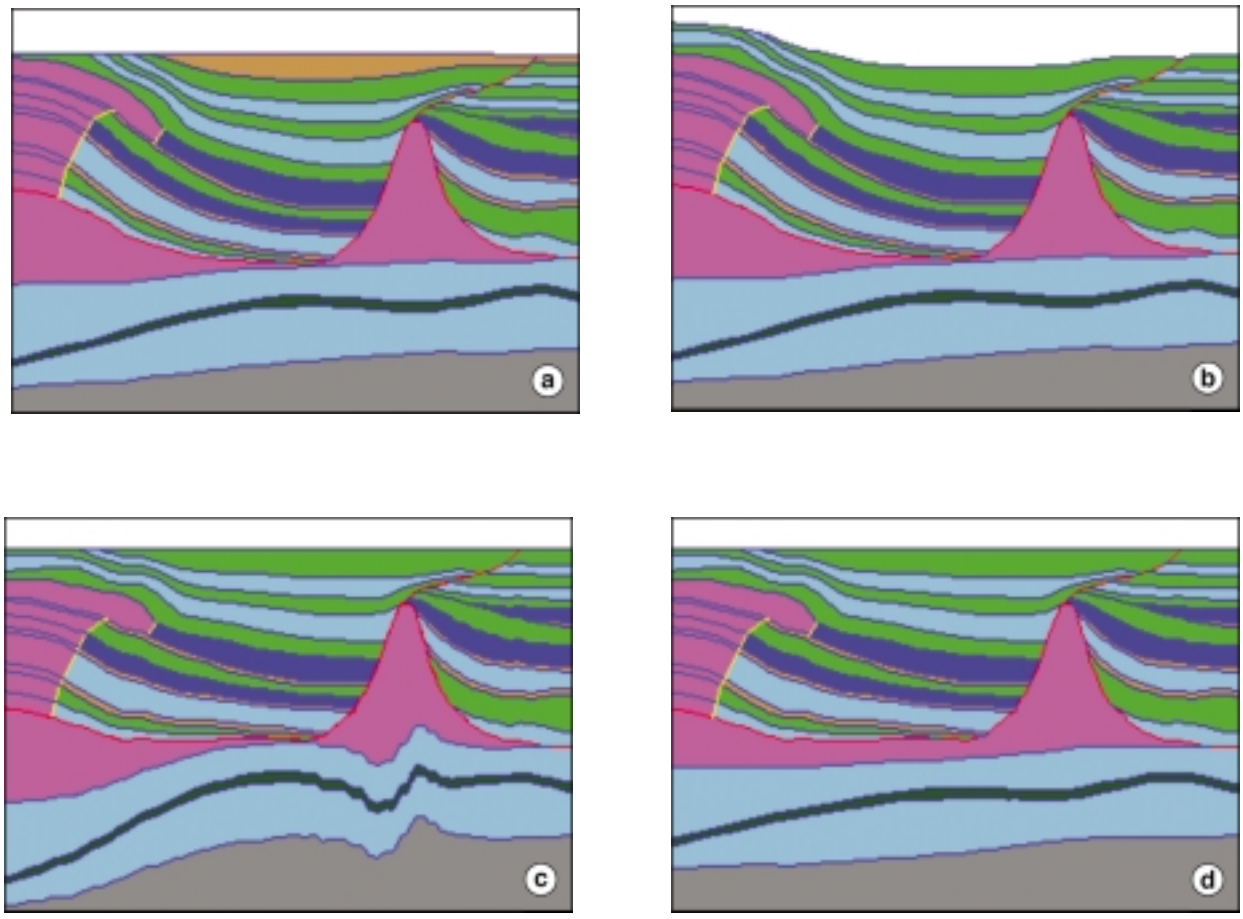

Figure 3
One restoration step characterized by: (a) the initial section at the beginning of the considered period; (b) the section after the edition of the eroded part, the stripping of the sedimented layer and the decompaction; (c) the section after the kinematic displacement; (d) the section after the thickness modifications.

branch of the tree. Each leaf of the branch is the section at the corresponding age. For each restoration, the backward process is composed of different steps.

The first step is the edition of the eroded parts if erosion has occurred during the considered period *(Fig. 3b)*. This edition may be helped by importing templates. The second step is an automatic popping of the section. Its allows taking off what has been sedimented during the considered period. Once the erosion and the sedimentation accounted for, the resulting section is decompacted using porosity depth relationships.

The backstripped section is then restored from a kinematics point of view *(Fig. 3c)*. At this stage, the displacements along faults are accounted using translations and vertical shear. As for the edition of the eroded parts, this operation may be constrained with the use of templates.

Once the section is restored, the last step of the backward process is the thickness modifications *(Fig. 3d)*. This step allows accounting for salt or mud tectonics. Correction of the edition of the erosion may be done at this stage. Nevertheless, the main use of this editor, is to account for thickness modifications due to salt tectonics or mud creeping.

These steps should be performed for each layer initially defined in the section at present day. The result is a scenario of restoration *(Fig. 4)* that should be validated against the previous structural study.

1.3 Forward Simulations

In these complex geometries, faults cut the basin into blocks that naturally define computational sub-domains. In the

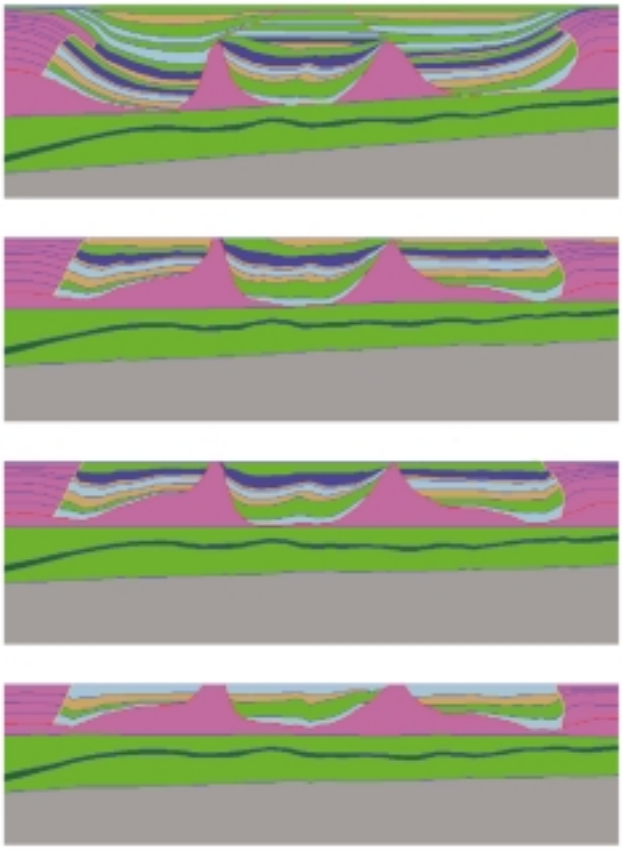

Figure 4
Resulting scenario at the end of the restoration.

blocks, the model accounts for the porous medium compaction, erosion, heat transfer, hydrocarbon formation *(see Appendix 2)* and migration *(Fig. 5)*. The equations are mass conservation of solid and fluids (water, oil, gas) coupled with the Darcy's law and a compaction law *(see Appendix 1)*. The faults have a constant thickness and their permeability may evolve with time. The prototype allows using three permeability models for the faults: faults may be impervious, pervious or may have a permeability that is a function of the neighboring lithologies and of the strain rate.

In order to solve the three-phase flow in a basin cut by faults along which block displacements can occur, Domain Decomposition Methods (DDM) are used (Willien *et al.*, 1998a, 1998b). The classical techniques used in the first version have been improved by using optimized interface conditions (Faille *et al.*, 2002). In these methods, the faults are considered as subdomains with their own geological properties. However, because of the very small width of the faults in comparison with the size of the basin we are studying another approach where the faults are characterized as interfaces between blocks (Faille *et al.*, accepted). In all the cases, the equations are discretized using a cell-centered finite volume scheme in space. Finite volume methods are known to be robust and cheap methods for the discretization of conservation laws in heterogeneous media and have the important property to be conservative.

Different time discretizations coupled with several DDM algorithms have been tested. In a first stage, a classical IMPES scheme (Implicitly advances the Pressure and Explicitly updates the Saturation in time) was used. But, it is well known that this scheme needs time step limitations for stability reasons. In order to use larger time steps, we have tested (Flauraud *et al.*, 2000) a sequential scheme, called IMPIMS (Implicitly advances the Pressure and Implicitly advances the Saturation in time). It consists in solving two nonlinear systems, one for the pressure (as in the IMPES scheme) and one for the saturation.

2 CASE STUDIES

This prototype has now been used to study petroleum systems all around the world. In the Bolivian foothills, were faults are supposed to be the most important carrier beds for hydrocarbon migration it has been used to perform a sensitivity study on fault permeability (Schneider *et al.*, 1999). In the Congo offshore, it has also been used to study the impact of faulting on maturity of the organic matter and hydrocarbon migration (Schneider *et al.*, 1999). In the Gulf of Mexico, it has been tested for studying the impact of the timing of salt withdrawal on hydrocarbon migration (Schneider *et al.*, 2000a).

More recently, Ceres has been tested within the frame of the *IFP* Subtrap consortium in thrust area such as the Canadian foothills and the Eastern Venezuelan foothills. The prototype has been used to quantify the fluid flow and to reconstruct the pore fluid history of the subthrust reservoirs. The use of Ceres implies a backward restoration. Although the backward restoration is fully appropriate for modeling an extensional basin well balanced (*e.g.* with Locace), it may turn difficult to constrain successive intermediate evolutionary stages, as far as the topography (prediction of erosion) and thrust geometry are concerned. In consequence, we have decided to use also the Thrustpack forward kinematic software to elaborate a better structural scenario. These successive intermediate geometries constructed with Thrustpack were then used as templates for the Ceres modeling.

2.1 Venezuelan Transect

As defined previously, the first work to perform at the beginning of a Ceres study is the definition of the initial

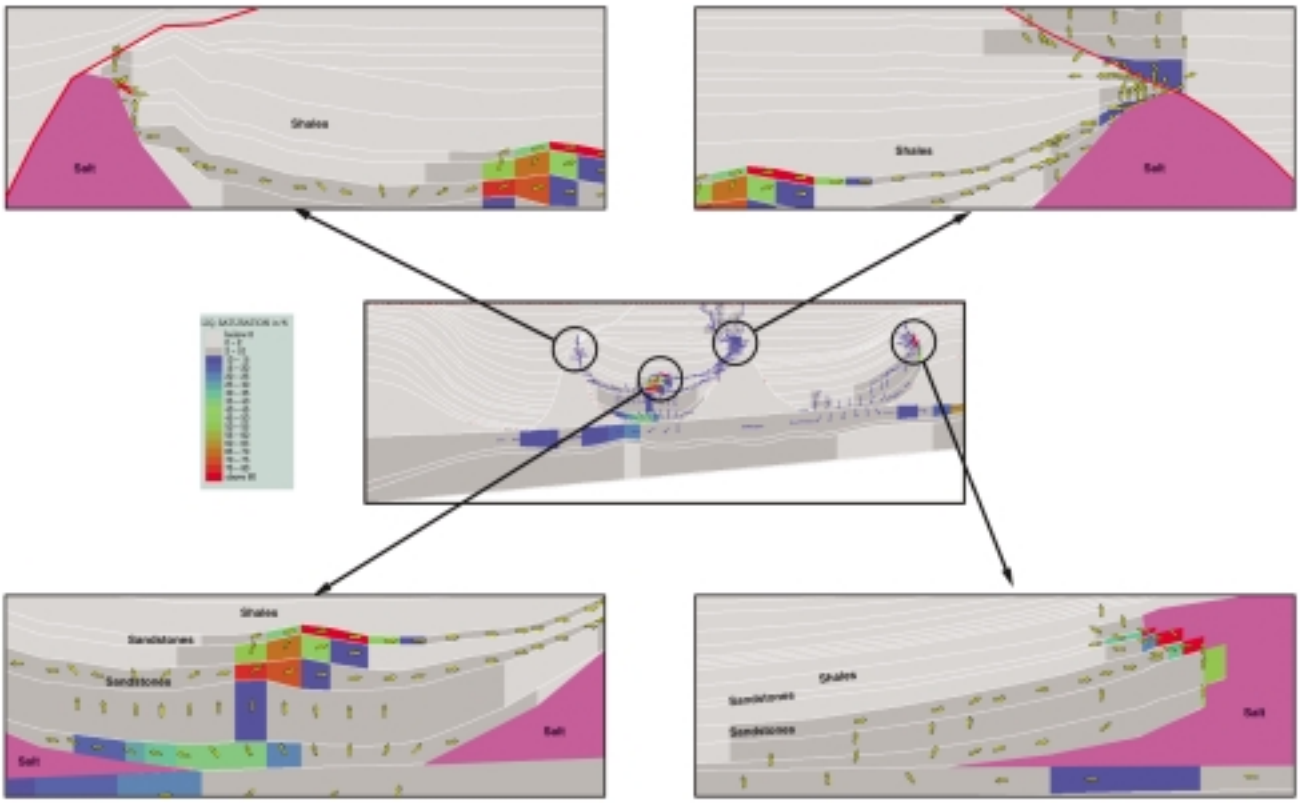

Figure 5

One example of hydrocarbon migration and distribution at present day.

section *(Fig. 6)*. This was done with data coming from the seismic interpretation, well data, field data, core data. Then, the available data and the Thrustpack scenario have been used to build the Ceres dataset.

From the data available, it is clear that the El Furrial structure is closed today as it is overpressured while the equivalent layers of the southern part have nearly hydrostatic pressures. The initial geometry *(Fig. 7a)* did not allow closing the El Furrial structure. Thus a second lithology distribution *(Fig. 7b)* has been defined by the introduction of a shaly layer at the top of the Oligocene. With this new geometry, the El Furrial structure that was not properly sealed in its northern part and in its southern part is now closed today at both sides.

The El Furrial trend from the Eastern Venezuelan transect displays two distinct episodes of quartz cementation. The first generation of quartz overgrowths, which account for more than 90% of the cements, is developed during the active dewatering processes in the Oligocene strata of the underthrust foreland. This is evidenced by the $\delta^{18}O$ signature and by the Ceres fluid flow simulations (Schneider *et al.*, 2001). In contrast, the second generation of quartz overgrowths displays quite distinct $\delta^{18}O$ values. These cements are originated when the deeper aquifer of the Lower Cretaceous Barranquin formation from the Pirital hanginwall started to expell its fluids towards the Oligocene reservoir of the adjacent El Furrial footwall unit. This is well evidenced by the Ceres fluid flow simulations (Schneider *et al.*, 2001).

2.2 Canadian Transect

As for the Venezuelan transect the first work to perform at the beginning of a Ceres study is the definition of the initial section *(Fig. 8)*. Then, one scenario for the geometry evolution has been defined *(Fig. 9)*. It is characterized by five major episodes in the geodynamic evolution:

- pre-flexural deposition during the Paleozoic and lower Mesozoic on a Precambrian substratum;
- deposition of synflexural formation from –100 Ma to –76 Ma;
- a main thrusting phase between –76 Ma and –55 Ma;
- a strong erosion from –55 Ma to –20 Ma;
- since –20 Ma the area is uplifted.

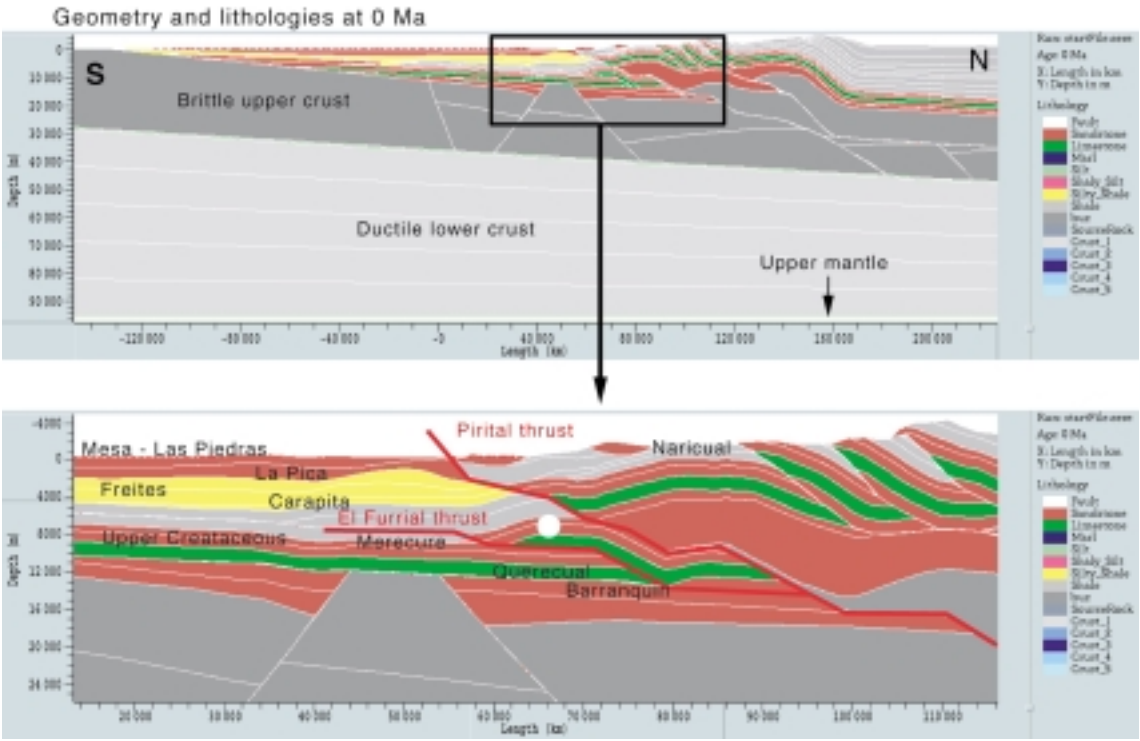

Figure 6

Geometry and lithology distribution of the Venezuelan section at present day. The white dot indicates the El Furrial structure.

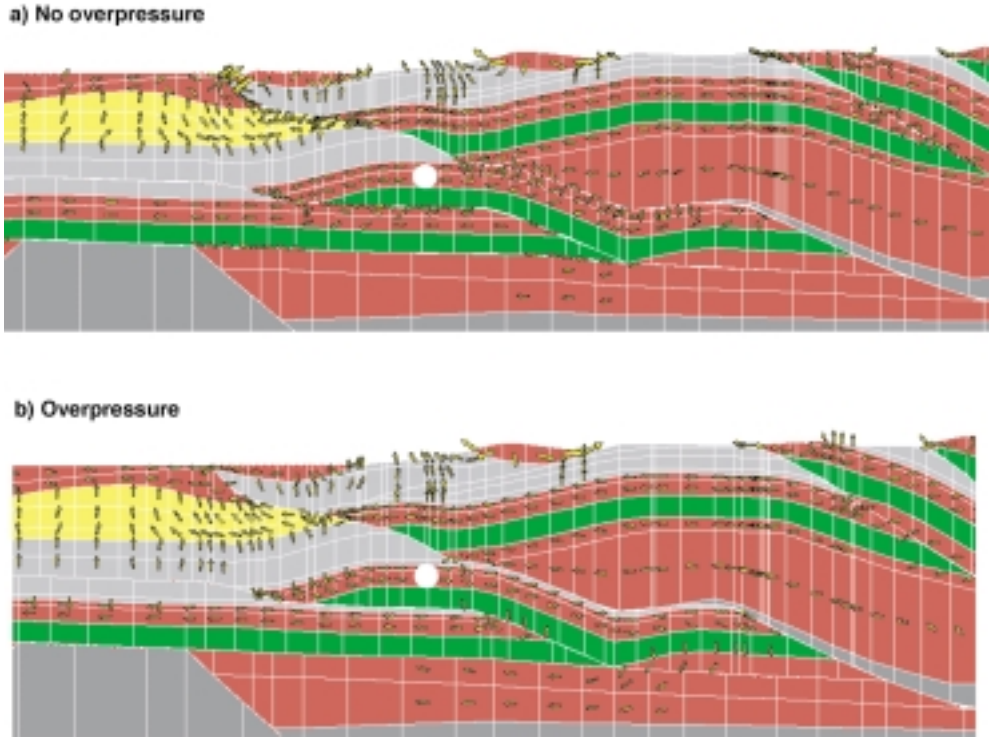

Figure 7

Initial lithology distribution (a) and new lithology distribution (b) where impervious sediments are involved in the El Furrial thrust. The white dot indicates the El Furrial structure.

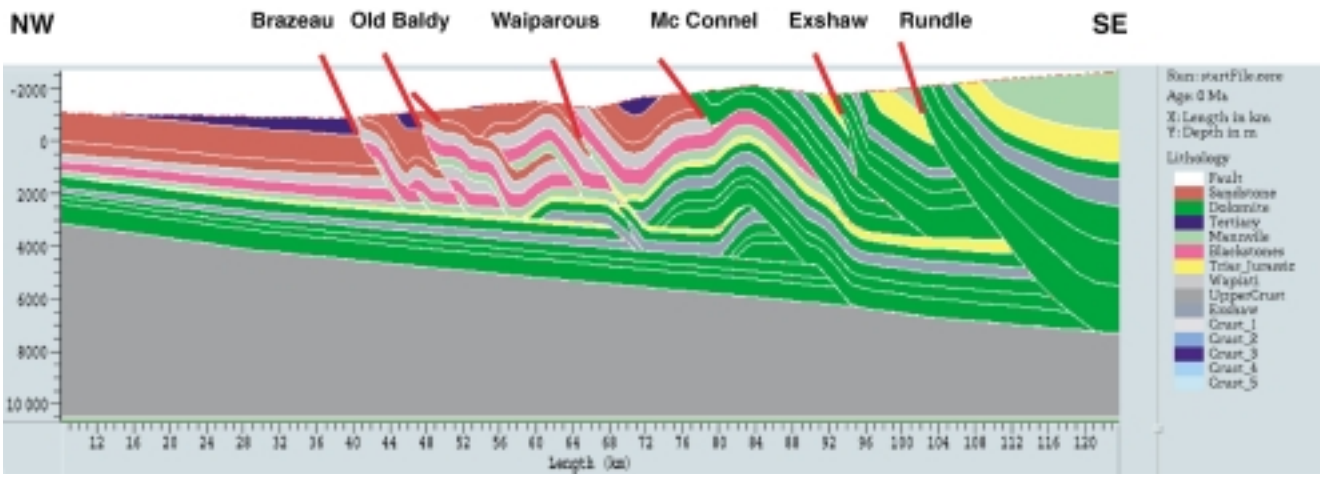

Figure 8

Geometry and lithology distribution of the Canadian section at present day.

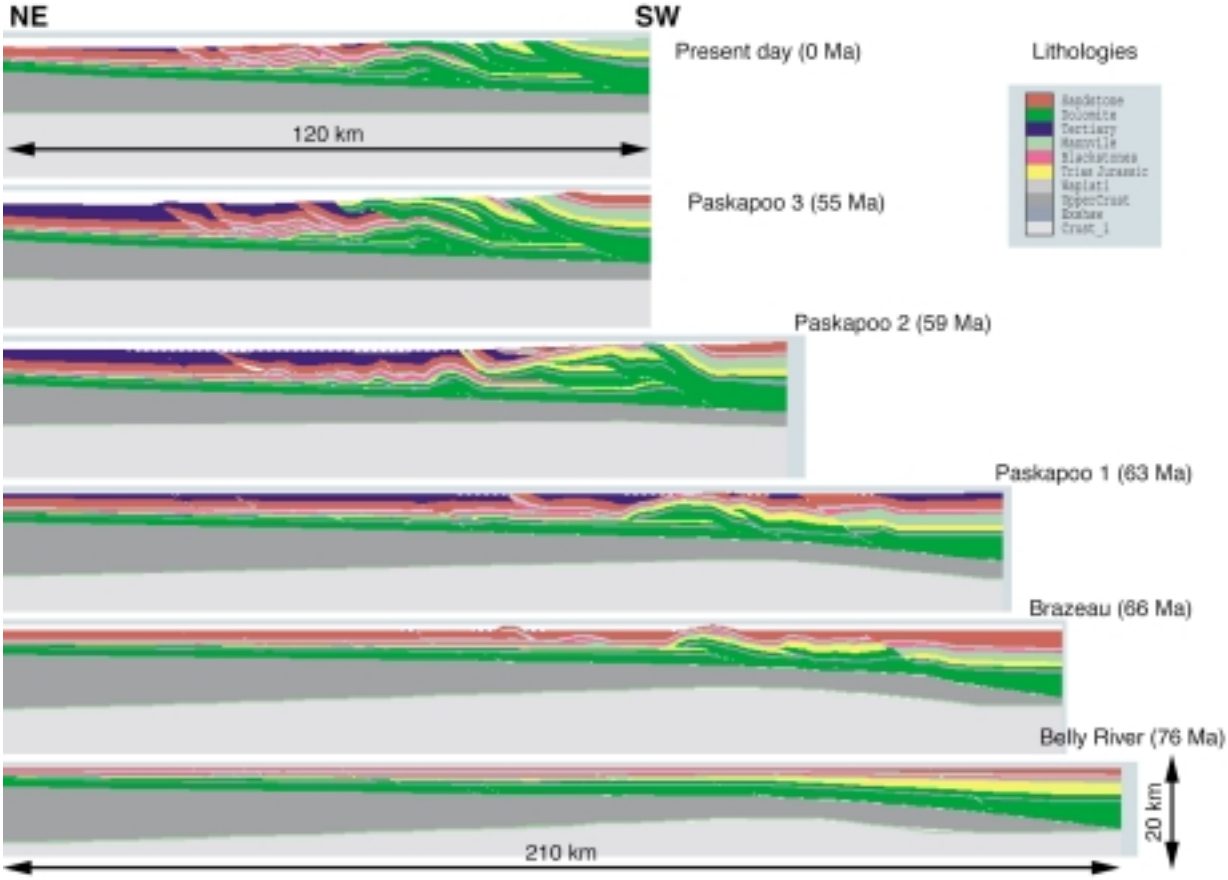

Figure 9

Geometrical evolution of the Canadian section from –76 Ma to present day.

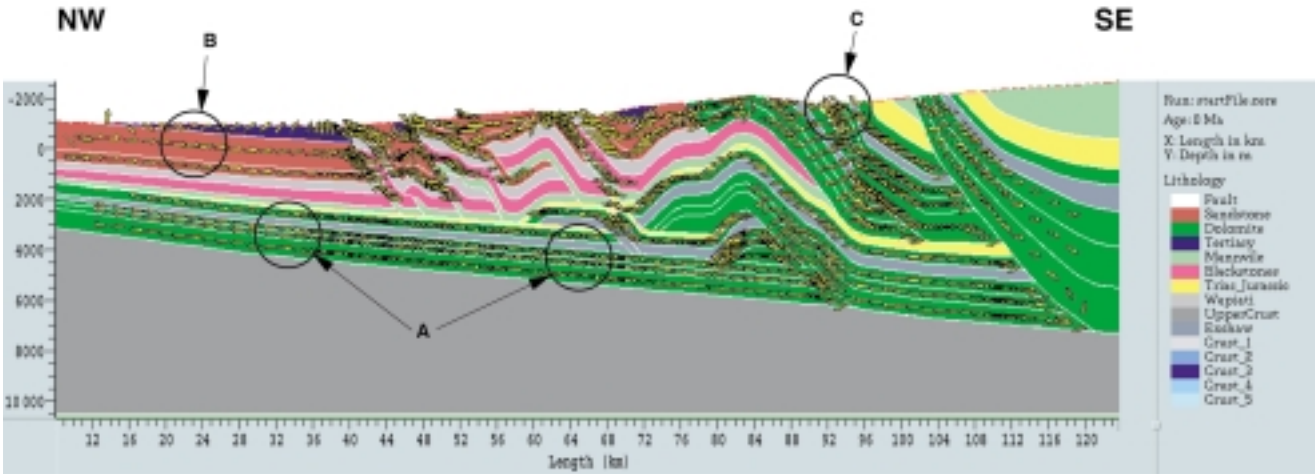

Figure 10

Canadian section at present day showing the computed fluid flow.

Unlike in Venezuela, where modern fluid flow is still controlled by the compressive evolution of the foothills, the Ceres fluid flow simulations shown that a dramatic change occurred since the end of the Laramian Orogeny. Indeed, more than 4 km of Mesozoic and Cenozoic series have been eroded and the hinterland and the foreland were progressively uplifted. Thus, the present day fluid flow is mainly controlled by the topography and the geometry of the aquifer *(Fig. 10)*.

CONCLUSION

Ceres is a new tool that enable to perform basin modeling in complex area where faults or salt tectonics may constrain the petroleum system. This prototype has been tested successfully worldwide. It may now be used to understand much more petroleum systems as the ones generally addressed with classical basin models.

The Ceres software, when coupled with a forward kinematics tool, such as Thrustpack, can be used for the simulation of the very complex structures of the foothills. It can provide reliable values for the velocity of the paleo-fluid circulations and for the paleo-fluid pressure.

It should be noticed that for these studies, it was of real importance to work closely with the structural geologists in order to define the initial section and the scenario for the kinematics restoration (Schneider *et al.*, 2002).

REFERENCES

Faille, I., Flauraud, E., Nataf, F., Schneider, F. and Willien, F. (2002) Optimized Interface Conditions for Sedimentary Basin Modeling. In Debit, N., Garbey, M., Hoppe, R., Periaux, J., Keyes, D. and Kuznetsov, Y., editors, *Proceedings of the Thirteenth International Conference on Domain Decomposition Methods*, 453-460, Lyon, France, 2000.

Faille, I., Flauraud, E., Nataf, F., Pégaz-Fiornet, S., Schneider, F. and Willien, F. (accepted) A New Fault Model in Geological Basin Modelling. Application of a Finite Volume Scheme and Domain Decomposition Methods. *Third International Symposium on Finite Volumes for Complex Applications — Problems and Perspectives*—June 24-28, 2002, Porquerolles, France.

Flauraud, E., Faille, I., Willien, F., Nataf, F. and Schneider, F. (2000) Implicit Scheme and Domain Decomposition Method for Multiphase Flow in Porous Medium. *Proceedings of the 7th European Conference on the Mathematics of Oil Recovery (ECMOR VII)*, Dino Hotel, Italy, September 5-8.

Lamoureux-Var, V. (1997) Modélisation de la compaction dans les bassins sédimentaires : approche mécanique. *Mémoire de thèse de doctorat de l'École polytechnique.*

Schneider, F. (1993) Modèle de compaction élastoplastique en simulation de bassins. *Revue de l'Institut Français du Pétrole*, **48**, 1, 3-14.

Schneider, F., Burrus, J. and Wolf, S. (1993) Modelling Overpressures by Effective-Stress/Porosity Relationships in Low-Permeability Rocks: Empirical Artifice or Physical Reality? In *Basin Modelling: Advances and Applications* edited by A.G. Doré *et al. NPF Special Publication*, 3, 333-341, Elsevier, Amsterdam.

Schneider, F., Potdevin, J.L., Wolf, S. and Faille, I. (1994) Modèle de compaction élastoplastique et viscoplastique pour simulateur de bassins sédimentaires. *Revue de l'Institut Français du Pétrole*, **49**, 2, 141-148.

Schneider, F., Potdevin, J.L., Wolf, S. and Faille, I. (1996) Mechanical and Chemical Compaction Model for Sedimentary Basin Simulators. *Tectonophysics*, **263**, 307-317.

Schneider, F., Devoitine, H., Faille, I., Flauraud, E. and Willien, F. (1999) A New 2D Basin Modeling Tool for HC Potential Evaluation in Faulted Area. Application to the Congo Offshore and to the Bolivian Sub Andean zone. *AAPG Hedberg Research Conference*, Colorado Spring, May 9-13.

Schneider, F., Faille, I., Flauraud, E. and Willien, F. (2000a) A 2D Basin Modeling Tool for HC Potential Evaluation in Complex Area. *62nd EAGE*, Glasgow, May 29-June 2.

Schneider, F., Wolf, S., Faille, I. and Pot, D. (2000b) A 3D-Basin Model for Hydrocarbon Potential Evaluation: Application to Congo Offshore. *Oil & Gas Science Technology – Revue de l'Institut Français du Pétrole*, **55**, 1, 3-13.

Schneider, F., Hernández, H. and Roure, F. (2001) Ceres Fluid-Flow and Pressure Modeling of an Eastern Venezuelan Transect. *AAPG Hedberg Conference "New Technologies and New Play Concepts in Latin America"*, November 4-9, 2001, Mendoza, Argentina.

Schneider, F., Faure, J.L. and Roure, F. (2002) Methodology for Basin Modeling in Complex Area: Examples from Eastern Venezuelan and Canadian Foothills. *AAPG Hedberg Conference "Deformation History, Fluid Flow Reconstruction and Reservoir Appraisal in Foreland Fold and Thrust Belts"*, May 14-18, 2002, Palermo - Mondello, Sicily, Italy.

Willien, F., Faille, I., Schneider, F. (1998a) Domain Decomposition Methods Applied to Sedimentary Basin Modeling. In Bjorstad, P.E., Espedal, M.S. and Keyes, D.E. Eds., *Ninth International Conference on Domain Decomposition Methods*, 736-744.

Willien, F., Faille, I., Nataf, F. and Schneider, F. (1998b). Domain Decomposition Methods for Fluid Flow in Porous Medium. *Proceedings of the 6th European Conference on the Mathematics of Oil Recovery (ECMOR VI)*, Peebles, GB, September 7-11.

Final manuscript received in June 2002

APPENDIX

1 PHYSICAL CONCEPTS AND MATHEMATICAL FORMULATIONS

The origin of the Eulerien coordinates system is given by the present sea level. The z axis is oriented downward.

Mass Balance Equations

For each phase $\alpha \in \{s, w, o, g\}$ (s = solid, w = water, o = oil, g = gas), the mass balance equation is:

$$\mathrm{div}\left(\phi_\alpha \rho_\alpha \overline{V}_\alpha\right) + \frac{\partial}{\partial t}\left(\phi_\alpha \rho_\alpha\right) = \rho_\alpha q_\alpha \qquad \text{(A1-1)}$$

ϕ_α is the volumetric fraction of the phase α, ρ_α is the density of the phase α, q_α is the source term corresponding to the phase α and $\overline{V}_\alpha$ is the mean velocity of the phase α. We have the following relationships:

$$\phi_s + \phi_w + \phi_o + \phi_g = 1 \quad \text{and} \quad \phi = \phi_w + \phi_o + \phi_g \qquad \text{(A1-2)}$$

where ϕ is the porosity of the porous medium. The momentum equation is simplified as follows:

$$\frac{\partial P_b}{\partial z} = \rho_b \, g \qquad \text{(A1-3)}$$

where P_b is the lithostatic pressure (weight of the sedimentary column), g is the gravity and ρ_b is the bulk density of the porous medium saturated by the fluids. This bulk density is given by:

$$\begin{cases} \rho_b = \phi_s \rho_s + \phi \rho_f \\ \rho_f = \dfrac{1}{\phi}\left(\phi_w \rho_w + \phi_o \rho_o + \phi_g \rho_g\right) = S_w \rho_w + S_o \rho_o + S_g \rho_g \end{cases} \qquad \text{(A1-4)}$$

where ρ_f is the mean density of the fluid and S_α is the saturation (volumetric fraction) of the phase α in the fluid. The energy equation (or heat equation) is:

$$\mathrm{div}\left(\sum_\alpha \left(\rho_\alpha \phi_\alpha C_\alpha T \overline{V_\alpha}\right) \pm \lambda_b \, \overline{\mathrm{grad}}(T)\right) + \frac{\partial}{\partial t}\left(\sum_\alpha \left(\rho_\alpha \phi_\alpha C_\alpha\right) T\right) = q_h \qquad \text{(A1-5)}$$

C_α is the heat capacity of the phase α, T is the temperature in Kelvin, λ_b is the bulk thermal conductivity of the porous medium saturated by the fluids α. It should be noticed that the mechanical energy dissipation is neglected. q_h represents the radiogenic source term and the heat source term related to thickness modification.

Fluid and Porous Medium Rheologies

The fluid is supposed to obey to the generalised Darcy's laws. Its mathematical formulation is for each of the phase ($\alpha \in \{w, o, g\}$):

$$\overline{U}_\alpha = \phi_\alpha\left(\overline{V}_\alpha \pm \overline{V_s}\right) = \pm \overline{\overline{k}} \eta_\alpha \left(\overline{\mathrm{grad}}(P_\alpha) \pm \rho_\alpha \overline{g}\right) \qquad \text{(A1-6)}$$

$\overline{U}_\alpha$ is the Darcy velocity of the phase α in the porous medium, $\overline{\overline{k}}$ is the intrinsic permeability tensor, η_α is the mobility of the phase α in the porous medium with respect to the other phases, and P_α is the pore pressure of the phase α.

The intrinsic permeability tensor is written as the product of an anisotropy tensor by the intrisic permeability:

$$\overline{\overline{k}} = \overline{\overline{a}} k(\phi) \quad \text{with} \quad \overline{\overline{a}} = \begin{bmatrix} a_{sx} & \\ & a_{az} \end{bmatrix} \qquad \text{(A1-7)}$$

The intrinsic permeability is computed with the modified Koseny-Carman's formula (Schneider *et al.*, 1996):

$$k(\phi) = \frac{0.2}{S^2} \frac{\phi^m}{\left(1 \pm \phi\right)^2} \qquad \text{(A1-8)}$$

where S is the specific surface area of the porous medium. m is an exponent, which generally equals 3. The mobility of the phase α is given by:

$$\eta_\alpha = \frac{kr_\alpha}{\mu_\alpha} \qquad \text{(A1-9)}$$

The fluid viscosities (water and hydrocarbons) are given by the Andrade formula:

$$\mu_\alpha(T) = \mu_\alpha^o \exp\left(b_\alpha\left(\frac{1}{T} \pm \frac{1}{T^o}\right)\right) \qquad \text{(A1-10)}$$

T is the temperature in Kelvin. The triphasic relative permeabilities are computed from the three two-phase couples of relative permeabilities by using the following formula:

$$\begin{aligned} (S_o + S_g) kr_w &= S_o kr_{wo}(S_w) + S_g kr_{wg}(S_w) \\ (S_w + S_g) kr_o &= S_w kr_{ow}(S_o) + S_g kr_{og}(S_o) \\ (S_o + S_w) kr_g &= S_o kr_{go}(S_g) + S_w kr_{gw}(S_g) \end{aligned} \qquad \text{(A1-11)}$$

Each of the relative permeability is given by:

$$\begin{aligned} S_\alpha \le Si_{\alpha\beta} \qquad & kr_{\alpha\beta} = 0 \\ Si_{\alpha\beta} < S_\alpha < 1 \quad & kr_{\alpha\beta} = \left(\frac{S_\alpha \pm Si_{\alpha\beta}}{1 \pm Si_{\alpha\beta}}\right)^{p_{\alpha\beta}} \end{aligned} \qquad \text{(A1-12)}$$

This original formalism has been developed for this model in order to be able to account for the possible symmetrical behaviour of each phase and to ensure numerical stability.

Compaction at basin scale and at geological time scale is supposed to be vertical. This choice is the result of a

compromise between accuracy and costs in term of cpu time (Lamoureux-Var V., 1997). The behaviour law is then given by a volumetric rheology (Schneider 1993; Schneider *et al.*, 1994, 1996):

$$\begin{cases} \dfrac{d_s\phi}{dt} & = \pm\beta(\sigma)\dfrac{d_s\sigma}{dt} \pm \alpha(\phi)\sigma \\ \beta(\sigma) & = \dfrac{\phi_a}{E_a}\exp\left(\pm\dfrac{\sigma}{E_a}\right) + \dfrac{\phi_b}{E_b}\exp\left(\pm\dfrac{\sigma}{E_b}\right) & \sigma \geq \sigma_m \\ \beta(\sigma) & = \dfrac{1}{E_e} & \sigma < \sigma_m \\ \alpha(\phi) & = (1 \pm \phi)\dfrac{1}{\mu_b(T)} & \sigma > 0 \text{ and } \phi > \phi^{\min} \\ \alpha(\phi) & = 0 & \sigma \leq 0 \text{ or } \phi \leq \phi^{\min} \\ \phi(t=0) = \phi_r + \phi_a + \phi_b \end{cases} \tag{A1-13}$$

where σ is the mean effective stress defined as follows:

$$\sigma = \left(\frac{1+2K_o}{3}\right)(P_b \pm bP_f) \tag{A1-14}$$

$$P_f = \frac{1}{\phi}\left(\phi_w P_w + \phi_o P_o + \phi_g P_g\right) = S_w P_w + S_o P_o + S_g P_g$$

where K_o is the ratio between the horizontal stress and the vertical stress, b is the effective stress coefficient (Schneider *et al.*, 1993) and P_f is the mean pore pressure. The pore pressure of each of the phases are related to each other by the capillary pressures.

$$\begin{cases} P_o = P_w + Pc_{ow} \\ P_g = P_w + Pc_{gw} \\ P_g = P_o + Pc_{go} \end{cases} \tag{A1-15}$$

If we make the assumption that the water phase is always present, this means that the porous medium is water wet, only the two first relations are necessary because we can write:

$$Pc_{go} = Pc_{gw} \pm Pc_{ow} \tag{A1-16}$$

By introducing the mean pore pressure, we obtain:

$$\begin{cases} P_w = P_f + Pc_{wf} \\ P_o = P_f + Pc_{of} \\ P_g = P_f + Pc_{gf} \end{cases} \quad \text{with} \quad \begin{cases} Pc_{wf} = \pm S_o Pc_{ow} \pm S_g Pc_{gw} \\ Pc_{of} = +S_w Pc_{ow} \pm S_g Pc_{go} \\ Pc_{gf} = +S_w Pc_{gw} \pm S_o Pc_{go} \end{cases} \tag{A1-17}$$

Under the assumption that water is always present, we can write:

$$\begin{cases} Pc_{wf} = \pm S_o Pc_{ow} & \pm S_g Pc_{gw} \\ Pc_{of} = +(1 \pm S_o) Pc_{ow} & \pm S_g Pc_{gw} \\ Pc_{gf} = \pm S_o Pc_{ow} & +(1 \pm S_g) Pc_{gw} \end{cases} \tag{A1-18}$$

As for the relative permeabilities, the three-phase capillary pressures are derived from the two-phase capillary pressures. With the assumption that water is always present, only the oil-water and the gas-water capillary pressure curves are necessary. They are given by the following formula:

$$\begin{array}{ll} \mathcal{S}_\alpha \leq Si_{\alpha\beta} & Pc_{\alpha\beta} = Pc1_{\beta\alpha} \\ Si_{\alpha\beta} < \mathcal{S}_\alpha < 1 \pm Si_{\beta\alpha} & Pc_{\alpha\beta} = Pc1_{\beta\alpha} \\ & \quad + (Pc1_{\alpha\beta} \pm Pc1_{\beta\alpha})\left(\dfrac{\mathcal{S}_\alpha \pm Si_{\alpha\beta}}{1 \pm Si_{\beta\alpha} \pm Si_{\alpha\beta}}\right)^{\gamma_{\alpha\beta}} \\ \mathcal{S}_\alpha \geq 1 \pm Si_{\beta\alpha} & Pc_{\alpha\beta} = Pc1_{\beta\alpha} \end{array} \tag{A1-19}$$

with: $\mathcal{S}_\alpha = \dfrac{S_\alpha}{S_\alpha + S_\beta}$ and $0 < \gamma_{\alpha\beta} \leq 1$.

State Equations

The density of each phase is supposed to be constant and is then given by: $\rho_\alpha = \rho_\alpha^o$.

Closure of the Problem

The problem consists in the resolution of a system composed of 13 equations with the 13 unknowns ϕ_α, $\overline{V}_\alpha$, P_α, T. Once the boundary conditions are given, the system is well posed.

Boundary Conditions

At the upper boundary, the pressures are imposed by the atmospheric pressure and by the bathymetry. The temperatures are imposed as a function of the altitude or function of the water depth.

At the lower boundary, there is no fluid flux and the displacements are imposed. The heat fluxes or the temperatures are imposed.

At the lateral boundaries, there is no heat flux and the displacements are only vertical. The fluid flux or the pressure may be imposed as a function of space and time.

2 HYDROCARBONS GENERATION

The hydrocarbon generation is performed with a conservative physical model which considers three components (oil, gas, and coke). In this model, the oil component is entirely in the hydrocarbon liquid phase, the gas component is entirely in the hydrocarbon vapour phase, and the water component is entirely in the water phase.

Description of the Porous Medium

The porous medium is composed of immobile components (solid, kerogen, and coke) and mobile components (oil, gas, water).

The porous medium is characterised by its initial composition *(see Table 1)*. We make the assumption that the initial existing components are the solid, the water and the kerogen. The initial porosity is given by the behaviour law *(see Appendix 1)*. The initial mass of kerogen is introduced by the TOC (Total Organic Content) which is given in gramme of organic carbon per gramme of dry rock. We admit that the TOC is given by the following formula:

$$\mathrm{TOC} = \frac{c\, M_k^o}{M_k^o + M_s^o} \qquad \text{(A2-1)}$$

where c is the mass carbon ratio of the kerogen that is a characteristic datum of the kerogen.

TABLE 1

Definition of the components
which constitute the considered porous medium

	Component	Density	Volumetric fraction	Volume	Mass
Immobile	Solid	ρ_s	$1-\phi$	$\mathrm{Vol}_s = \mathrm{Vol}_b(1-\phi)$	$M_s = \mathrm{Vol}_s \rho_s$
	Kerogen	ρ_k	ϕS_k	$\mathrm{Vol}_k = \mathrm{Vol}_b \phi S_k$	$M_k = \mathrm{Vol}_k \rho_k$
	Coke	ρ_c	ϕS_c	$\mathrm{Vol}_c = \mathrm{Vol}_b \phi S_c$	$M_c = \mathrm{Vol}_c \rho_c$
Mobile	Oil	ρ_o	ϕS_o	$\mathrm{Vol}_o = \mathrm{Vol}_b \phi S_o$	$M_o = \mathrm{Vol}_o \rho_o$
	Gas	ρ_g	ϕS_g	$\mathrm{Vol}_g = \mathrm{Vol}_b \phi S_g$	$M_g = \mathrm{Vol}_g \rho_g$
	Water	ρ_w	ϕS_w	$\mathrm{Vol}_w = \mathrm{Vol}_b \phi S_w$	$M_w = \mathrm{Vol}_w \rho_w$

Primary Cracking

During the primary cracking, the kerogen is transformed with n parallel reactions, into oil, gas and coke.

$$\text{Kerogen}\begin{cases} x_1 \rightarrow \alpha_1^o \text{ oil} + \alpha_1^g \text{ gas} + \alpha_1^c \text{ coke} \\ \vdots \rightarrow \vdots + \vdots + \vdots \\ x_i \rightarrow \alpha_i^o \text{ oil} + \alpha_i^g \text{ gas} + \alpha_i^g \text{ coke} \\ \vdots \rightarrow \vdots + \vdots + \vdots \\ x_n \rightarrow \alpha_n^o \text{ oil} + \alpha_n^g \text{ gas} + \alpha_n^c \text{ coke} \end{cases} \qquad \text{(A2-2)}$$

x_i is the normalised partial potential of reaction i. It is a datum of the kerogen which obeys to the following relation: $\sum_{i=1}^{n} x_i^0 = 1$. α_i^o (respectively α_i^g and α_i^c) is the oil (respectively the gas and coke) quantity produced by reaction i. We have: $\alpha_i^o + \alpha_i^g + \alpha_i^c = 1$.

Each of these elementary reactions are supposed to be controlled by a first order kinetic given by the following equation:

$$\frac{dx_i}{dt} = \pm k_i\, x_i \quad \text{with} \quad k_i = A_i\, e^{\pm \frac{E_j}{RT}} \qquad \text{(A2-3)}$$

A is the frequency factor. E is the activation energy. R is the perfect gas constant. T is the temperature in Kelvin.

Secondary Cracking

The oil produced by the primary cracking is then transformed, during the secondary cracking, into gas and coke. This reaction is supposed to be controlled by a first order kinetic given by the following equation:

$$\text{Oil} \rightarrow \beta_o^g \text{ Gas} + \beta_o^c \text{ Coke} \qquad k_o = A_o\, e^{-\frac{E_o}{RT}} \qquad \text{(A2-4)}$$

β_o^g and β_o^c are the stoechiometric coefficients of the reaction which respect the following condition: $\beta_o^g + \beta_o^c = 1$.

Transformation Ratio

The equations which described the primary cracking are discretized with an implicit scheme for the partial potential and with explicit temperatures. Thus, we have:

$$\frac{dx_i}{dt} = -k_i\, x_i \Rightarrow x_i^{m+1} = \frac{x_i^m}{1 + k_i^m\, \delta t} \qquad \text{(A2-5)}$$

δt is the time step. The m exponent indicates values taken at t, while the m+1 exponent indicates values taken at $t + \delta t$. The transformation ratio (TR) of the organic mater is then given by:

$$\mathrm{TR} = 1 - \sum_{i=1}^{n} x_i^{m+1} \qquad \text{(A2-6)}$$